Fault-Tolerant RFID Reader Localization Based on Passive RFID Tags

Weiping Zhu*, Jiannong Cao*, Yi Xu†, Lei Yang*, and Junjun Kong*
*Department of Computing, The Hong Kong Polytechnic University, Hong Kong
†Department of Applied Mathematics, The Hong Kong Polytechnic University, Hong Kong
*{csweizhu, csjcao, csleiyang, csjkong}@comp.polyu.edu.hk †amayixu@yahoo.com.hk

***Abstract*—With the growing use of RFID-based devices, RFID reader localization attracts increasing attentions recently. In this technology, an object carrying an RFID reader is located by communicating with some passive RFID tags deployed in the environment. One important problem of RFID reader localization is that frequent occurred RFID faults affect localization accuracy. Specifically, complex localization environment (may include metal, water, obstacles, etc.) makes some tags fail to communicate with the reader, which makes the localization result deviate from the real location. Existing approaches can tolerate the faults occurred in individual tags and lasting for a short time period, but suffer serious localization error if the faults exist in a large region and last for a long time period. Moreover, existing approaches do not provide quality measurement of a localization result. In this paper, we propose an effective fault-tolerant RFID reader localization approach suitable for the above-mentioned situations, and illustrate how to measure the quality of a localization result. We have taken extensive simulations and implemented an RFID-based localization system. In both cases, our solution outperforms existing approaches in localization accuracy and can provide additional quality information.**

I. Introduction

Radio Frequency Identification (RFID) is an identification technology that employs radio waves to transfer the identity information stored in RFID tags to RFID readers. The most widely used RFID tag is the passive RFID tag which has no embedded battery but is just powered by the radio waves sent from RFID readers. With the growing use of RFID-based devices, many researchers are interested in utilizing RFID to provide localization service [1], [2], [3], [4], [5]. Compared with the devices used in other localization technologies, passive RFID tag is of tiny size and low cost hence quite suitable for large-scale deployment. In this paper, the tag refers to the passive RFID tag.

RFID-based localization can be classified into *tag localization* and *reader localization* [6]. In the tag localization as shown in Fig. 1(a), each object to be located is attached with an RFID tag and RFID readers are scattered in the environment. A server gathers data from the readers, executes a localization algorithm and notifies the result to the object. On the contrary, in the reader localization as shown in Fig. 1(b), the object carries an RFID reader and a set of RFID tags are deployed in the environment. The object uses the reader to actively obtain its own location. Compared with tag localization, reader localization reduces infrastructure cost by using cheap tags instead of expensive readers. Moreover, unlike tag localization with centralized computing, reader localization is inherently distributed and more scalable. We focus on the reader localization in this paper.

We target the applications which provide localization service in a large region (e.g. a shopping mall, a warehouse, etc.), where the infrastructure provider cannot afford expensive RFID readers or on-site maintenance which may disturb normal operations. Instead, the infrastructure provider can place a collection of cheap passive RFID tags in the region, and install readers at the user side (e.g. at shopping carts, forklifts, etc.). The readers are of a relative small number and easier to maintain. With the advance of RFID devices, we even can expect that a human being takes a phone-size RFID reader for localization in the future.

One fundamental problem of reader localization is how to handle the faults frequently occurred in the localization process. The faults can be caused by complex radio propagation, environment interference or hardware failures. Many researchers have noticed this and proposed some countermeasures utilizing spatial/temporal redundancy [2], [7], [8]. A tag's fault can be corrected by its neighboring tags or through multiple tag readings. However, these approaches cannot work in the situation that faults exist in a large region and last for a long time, which is called *long-lasting regional fault* in this paper. Unfortunately, this kind of fault is not uncommon in RFID applications. For example, an object to be located happens to be near a metal equipment. Due to shielding effect, all the tags around the metal equipment cannot respond to the reader during the whole localization process. One more example is the localization near walls, corners or other objects. It is difficult to locate the target object in such circumstance since the identification region is deformed and quite different from that in the open region [4]. Long-lasting regional fault

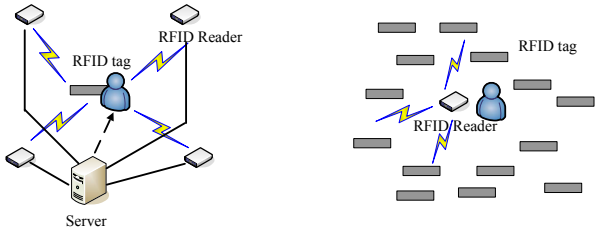

(a) tag localization (b) reader localization

Fig. 1. RFID-based localization

causes serious localization error if not carefully considered.

Another problem of existing approaches is that they do not provide quality measurement of the localization result. Since RFID faults occur frequently and the causes are complex in most of applications, a measurement representing the confidence of the localization result is important for the user. When the quality of a localization result is below a threshold, the user can take further actions.

In this paper, we firstly formally describe the categories of RFID faults in RFID reader localization. Then we propose an approach which is tolerant of long-lasting regional fault utilizing geometric knowledge of the identification region and linear second-order cone programming. We measure the quality of a localization result using *quality index* defined by us. Extensive simulations and a real system are used to validate the effectiveness of our approach. In summary, this paper makes the following specific contributions.

- We formally describe the categories of RFID faults in RFID reader localization.
- We propose an effective localization approach which can tolerate long-lasting regional fault.
- We propose quality index to measure the quality of a localization result obtained by our approach.

The rest of the paper is organized as follows: Section II reviews related works. Section III describes the problem and the system model. Section IV describes our solution. Simulation and experiment results are reported in section V and section VI respectively. Finally, section VII concludes the paper.

II. Related Works

Most of the works related to RFID reader localization utilize a geometric and range-free method to localize the target object. In [9], the authors proposed a low cost outdoor localization method based on radio communication. A set of devices are deployed in the environment as reference nodes and transmit beacon signals periodically. The target object receives the signals and locates itself to be the centroid of proximate reference nodes. In APIT [10], the target object interacts with neighboring objects to determine whether it is in a triangle formed by every three reference nodes. It iteratively narrows the possible region in which the target object resides. The centroid of the possible region is considered as the location of the target object. This method is useful in the scenario with multiple readers which can interact with each other, rather than one reader scenario in this paper. In virtual landmark [3], the authors did not use real reference tags but virtual reference tags. Based on the constraints that a reader can detect the tag or not, the method filters out corresponding virtual reference tags and then computes the centroid. In [8], the authors improved the centroid method to a weighted centroid method integrating RSSI(Received Signal Strength Indicator) as the weight of reference nodes. With a little difference, LANDMARC [7] uses a hybrid deployment where both readers and reference tags are deployed as the infrastructure. When a target object comes into a reader's identification region, k nearest tags are selected to calculate the weighted centroid as the localization result. The weight of a reference tag is inversely proportional to the similarity in RSSI between it and the target tag. In [2], the authors also use weighted centroid method but the weights are defined by a Gaussian function. In [4], the author proposed a non-linear programming method to locate the reader based on the geometric knowledge of the identification region in 3D space. In [11], the affect of different tag placements on localization are discussed. Early works of centroid method did not consider much about the fault-tolerance problem. Later works [2], [7], [8] considered RFID faults and utilized spatial/temporal redundancy to select the most reliable tags and filter out the others. However, all existing works are not capable of coping with long-lasting regional fault during the localization process. We aim to address this problem in this paper.

Rather than the geometrical method, researchers also developed some localization methods based on machine learning. In [12], the target object firstly walks through every labeled location in a region to record the RSSI as the fingerprint. In the normal operation, the measured RSSI is matched with recorded fingerprints. The location of the most similar fingerprint is returned as the location of the target object. The probabilistic measurement model is further combined into the method to improve localization accuracy [5]. In [13], the authors use Support Vector Machine to carry out the training and matching. The machine learning method needs a time-consuming training phase and a large database. For many applications, this may not be practical so we do not consider this method in this paper.

III. System Model

We firstly describe the localization model used in this paper. Then we discuss the categories of RFID faults in RFID reader localization.

A. RFID-Based Localization

For consistency, we use a system model similar to [3], [4]. As shown in Fig. 2, a hexahedron (i.e. a warehouse, a reading room, etc.) has the length, width and height of L, W, H respectively. A set of reference tags are deployed in the floor and the ceiling of the hexahedron. The reference tags are placed in a grid with the spacing of d (d is large enough to avoid near-field effect among tags). With an arbitrary coordinate system, the coordinates of the reference tags are known in advance. A target object carrying an RFID reader is in the hexahedron and needs to be located. The identification region of the reader is assumed to be a sphere. When projected on the ceiling/floor, the identification region is a circle with the radius of r. We refer the projected identification region in an ideal environment as *ideal identification region* in this paper. The localization depends on RFID identification process, in which the tags detected successfully by the reader are called *activated tags* and the others are called *un-activated tags*. The activated tags having both activated tags and un-activated tags as neighbors are called *border tags*. The environment is not assumed perfect and faults occur frequently.

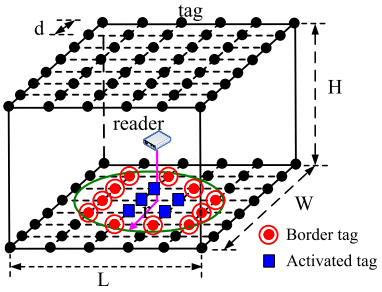

Fig. 2. RFID-based localization model

There are two objectives in our problem: 1) to locate the target object with minimum error; 2) to provide quality measurement of the localization result to the user.

Several issues need to be emphasized. Firstly, this model is applicable to both 2D and 3D localization. In 2D localization, it is tailored to have reference tags only in the ceiling or in the floor, but not both. Secondly, sphere identification region is not necessary. We firstly assume this for convenience in discussion and relax it in section IV-F. Finally, our approach does not need radio signal strength information. The reader only provides the information which tags are detected.

B. RFID Faults

The RFID faults are classified into two categories: *unintended reading* and *missing reading*. As shown in Fig. 3(a), the unintended reading means that the tags outside the ideal identification region are read while the missing reading means that the tags in the ideal identification region are not read.

For the unintended reading, the solution is based on the assumption that the further a tag is from the reader, the lower probability it is detected. By reading the tags for multiple times [8], [9], or assigning different weights to the tags [2], [7], the effect of unintended reading (especially the readings far from the ideal identification region) can be effectively eliminated.

The missing readings are further classified in temporal dimension and spatial dimension. In temporal dimension, there are *intermittent fault* and *long-lasting fault*. In spatial dimension, there are *spot fault* and *regional fault*. The combination of long-lasting fault and regional fault is called *long-lasting regional fault*, which denotes that faulty tags occur in a region and fail to respond to the reader in a continuous time duration.

If the fault is not a long-lasting regional fault, it can be handled similarly by above-mentioned multiple reading method utilizing spatial/temporal redundancy. However, long-lasting regional fault is difficult to deal with because the fault is continuous in both spatial dimension and temporal dimension. Unfortunately, this fault is not rare in the RFID applications. In this paper, long-lasting regional fault is our major concern. Specifically, we assume that tag faults last during the whole identification process. And in the rest of this section, we discuss more about the regional fault.

In the localization process, we use activated tags to infer the reader's identification region. We define *activated region* to denote the inferred region:

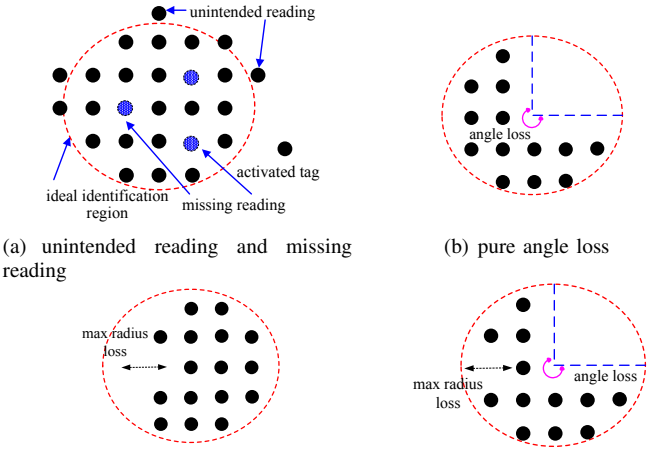

(a) unintended reading and missing reading

(b) pure angle loss

(c) pure radius loss

(d) mixed loss

Fig. 3. Different RFID faults in the localization process

Definition 1 (activated region): Given an activated tag set A, the activated region inferred by A is defined as the convex hull of the activated tags, denoting as $conv(A)$.

Due to RFID faults, some tags may not be identified, so the activated region may be different from the ideal identification region. We build a polar coordinate system with the pole of the reader. Observing the difference between the ideal identification region and the activated region, there are three basic types of regional fault: *pure angle loss*, *pure radius loss* and *mixed loss*. More complex faults are the combinations of them. Fig. 3(b) to 3(d) show the examples and the formal definitions are as follows.

Definition 2 (pure angle loss): Compared with ideal identification region $\rho = \phi(\theta)(0 \leq \theta \leq 2\pi)$, an activated region with pure angle loss is defined as $\rho = \phi(\theta)(\theta' \leq \theta \leq \theta'', 0 \leq \theta' \leq \theta'' \leq 2\pi)$. The angle loss is defined as $2\pi - (\theta'' - \theta')$.

Definition 3 (pure radius loss): Compared with ideal identification region $\rho = \phi(\theta)(0 \leq \theta \leq 2\pi)$, an activated region with pure radius loss is defined as $\rho = \phi'(\theta)(0 \leq \theta \leq 2\pi, 0 < \phi'(\theta) \leq \phi(\theta))$. The max radius loss is defined as $max_\theta(\phi(\theta) - \phi'(\theta))$.

Definition 4 (mixed loss): Compared with ideal identification region $\rho = \phi(\theta)(0 \leq \theta \leq 2\pi)$, an activated region with mixed loss is defined as $\rho = \phi'(\theta)(\theta' \leq \theta \leq \theta'', 0 \leq \theta' \leq \theta'' \leq 2\pi, 0 < \phi'(\theta) \leq \phi(\theta))$. The angle loss is defined as $2\pi - (\theta'' - \theta')$ and the max radius loss is defined as $max_\theta(\phi(\theta) - \phi'(\theta))$.

IV. Solution

In this section, we introduce our approach which is tolerant of long-lasting regional fault. Then we analyze the performance of this approach in different situations.

A. Basic Method

In the ceiling/floor of the hexahedron, the ideal identification region is a circle centered with the reader. The purpose of localization is to find the circle center with the help of activated tags. The tags are processed firstly to filter out the unintended reading. Then we discuss the missing reading as follows.

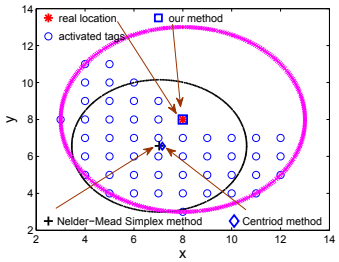

Fig. 4. An example to illustrate the difference between ATI and existing approaches. There is a regional fault with angle loss of $3\pi/4$.

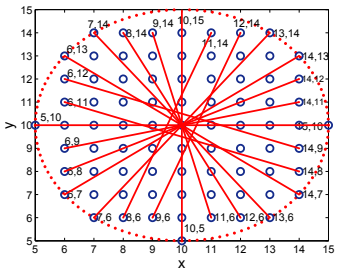

(a) ideal identification region

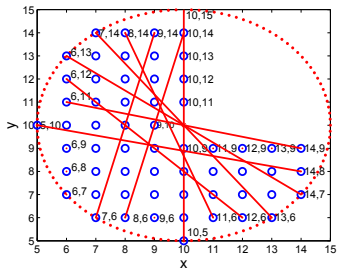

(b) angle loss of $\pi/2$

Fig. 5. Key pairs and quality index in a) ideal identification region b) an activated region with pure angle loss. Two tags connected by a line form a key pair. Quality index is defined as the number of key pairs.

In previous works such as Nelder-Mead Simplex method [4] and centroid method [3], [7], the activated region is just viewed as the reader's ideal identification region. The tags with intermittent fault or spot fault are corrected into activated tags using spatial/temporal redundancy. However, it cannot work in the presence of long-lasting regional fault. As a result, the localization result deviates from the real location, as shown in Fig. 4. To overcome the drawback, we propose a method which includes all activated tags in the ideal identification region. We call this method ATI (Activated Tag Included method). ATI fully utilize the geometric knowledge of the identification region hence has a better performance.

Let activated tags have the coordinates $\{(x_i, y_i) \mid i = 1...n\}$. We formally describe ATI as following:

$$\begin{aligned} &min\ r_f \\ &st.\ (x_i - x_f)^2 + (y_i - y_f)^2 \le r_f^2 \quad (i = 1...n) \end{aligned} \tag{1}$$

The above formulation can be transformed to be a linear second order cone programming. Let us define the variables:

$$\bar{x}_i = x_i - x_f, \bar{y}_i = y_i - y_f, \bar{r}_i = r_i, w_i = (\bar{x}_i, \bar{y}_i, \bar{r}_i)^T$$

Then we have a new formulation:

$$\begin{aligned} min \quad & r_f \\ st. \quad & [0,0,1]w_i = r_f \\ & \begin{pmatrix} 1 & 0 & 0 \\ 0 & 1 & 0 \end{pmatrix} w_i = \begin{pmatrix} x_i - x_f \\ y_i - y_f \end{pmatrix} \\ & w_i \in (\bar{x}_i^2 + \bar{y}_i^2 \le r_f^2) \end{aligned} \tag{2}$$

We obtain the result using SDPT3 4.0 [14] which is a well-known Matlab software package to solve linear second order cone programming problem.

An example is shown in Fig. 4. The reader's location is of a great deviation when determined by Nelder-Mead Simplex method or centroid method, but quite accurate when determined by ATI.

B. Accuracy Analysis in Pure Angle Loss

We analyze the effectiveness of ATI in the presence of pure angle loss. There are three theorems as the basic results. We assume the radius of the ideal identification region is r.

Theorem 1: In pure angle loss, if the angle loss is less than π, the circle determined by ATI has the radius at least r.

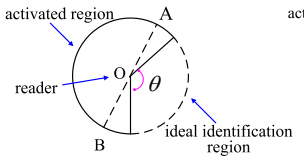

(a) angle loss $\theta < \pi$

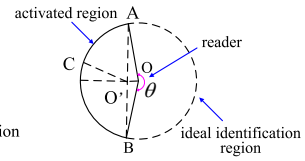

(b) angle loss $\theta \ge \pi$

Fig. 6. Different situations in pure angle loss

Proof: As shown in Fig. 6(a), the activated region is a circular sector, and the angle loss is θ. Since $\theta < \pi$, we always can find a diameter AB of the ideal identification region included in the activated region. $|AB| = 2r$. When ATI determines a circle with minimal radius say r' including all activated tags, point A and B must be included in that circle. According to the property that the length of a diameter is the maximal length between any two points in the circle, we have $2r' \ge |AB| = 2r$, so $r' \ge r$. ■

Theorem 2: In pure angle loss, if the angle loss is greater than or equal to π, a circle with the center rather than the reader's exact location and the radius less than r can be found as a feasible solution of ATI.

Proof: As shown in Fig. 6(b), the circular sector $\widehat{AOB}$ is the activated region and the angle loss is θ. Since $\theta \ge \pi$, we connect point A and B using a line and get the middle point O' as the new circle center. We have $|AO'| = |BO'| < |AO| = r$. For an arbitrary point C in arc AB, we also have $|CO'| < r$. So at least we can find a circle with the center of O' and the radius less than r to include all activated tags. ■

Theorem 3: In pure angle loss, ATI can determine the reader's exact location if and only if the angle loss is less than π.

Proof: if the angle loss is less than π, according to Theorem 1, ATI determines a circle whose radius is at least r. Considering that the reader's exact location is also a candidate of the circle center, ATI finally returns a circle centered at the reader's exact location and with the radius of r. On the other side, if ATI can determine the reader's exact location, we can prove the statement that the angle loss is less than π by contradiction. Assuming that the angle loss is no less than π, according to Theorem 2, we can find a circle whose center is not the reader's exact location as the solution. This contradicts the precondition that the reader's exact location can be determined. ■

Algorithm 1: Quality Index Algorithm

```
1  qualityIndex = 0
2  put all border tags in N
3  foreach A ∈ N do
4  |  find the tag B such that |AB| is maximal (B ∈ N)
5  |  if |AB| == 2r then
6  |  |  remove A and B from N
7  |  |  qualityIndex++
8  |  end
9  endfch
10 return qualityIndex
```

C. Quality Index in Pure Angle Loss

From previous analysis, the accuracy of a localization result depends on the angle loss. In fact, the angle loss can be viewed equivalently in another way. We observe how many diameters of the ideal identification region still exist in the activated region. As shown in Fig. 6(a), when $\theta < \pi$ (θ is the angle loss), we always can find a diameter of this kind in the activated region; while as shown in Fig. 6(b), when $\theta \geq \pi$, we cannot do that. When the angle loss is less, we can find more diameters and vice verse. Motivated by this, we propose to measure the quality of a localization result by the number of diameters of this kind found in the activated region. We define quality index of a localization result as follows:

Definition 5 (key pair): In a localization process, two activated tags are defined as a key pair if they are the end points of a diameter of the ideal identification region.

Definition 6 (quality index): The number of key pairs is defined as the quality index of a localization result.

An example of key pairs and quality index is shown in Fig. 5. We use quality index to measure the confidence of a localization result with pure angle loss. Intuitively this is reasonable since quality index denotes angle loss.

We designed Algorithm 1 to calculate the quality index. Firstly the algorithm initiates *qualityIndex* to 0 and obtains all border tags in N (line 1-2). For each tag in N, say A, a process (line 3-9) is run as follows. The algorithm firstly finds a tag B which has the maximum distance from A (line 4). Then the distance is compared with $2r$. If the equality holds, these two tags form a key pair. Remove these two tags and increase *qualityIndex* (line 5-8). Since the diameter is the maximum distance between two points in a circle, the correctness and convergence of this approach are easy to prove. The worst time complexity of this algorithm is $O(n^2)$.

D. Considering Grid Placement

In previous two sub-sections, we discussed the solution in theory and assumed that the border of ideal identification region can be perfectly inferred by the border tags. This assumption only holds in quite dense placement of tags. However, this placement is not practical because not only the tag cost is high, but the near-filed effect among tags can no longer be ignored and affect the radio transmission. In our model, we place the tags in a grid with constant spacing. The spacing causes errors in the localization result and the quality index. Here we discuss these errors.

We firstly compare the border tags with the real border of ideal identification region. The difference is the error in a localization result caused by grid placement. We have Theorem 4 (proof omitted but will be validated by simulations).

Theorem 4: The error of a localization result of ATI in the grid placement, is always less than d. And the relative error is always less than d/r.

We focus on the error of quality index caused by grid placement. Since the border tags may deviate from the border of ideal identification region, the diameters determined by Algorithm 1(line 4) may be shorter than $2r$. We call this kind of diameter *degraded diameter*. In the following, we calculate the lower bound of a degraded diameter's length and then revise Algorithm 1 to take this into account.

At first glance, the length of the shortest degraded diameter seems to be $(2r - 2d)$. However, this is not true. As shown in Fig. 7(c), when a border tag A finds its partner say B to form a key pair, B may deviate from the ideal location B' due to the spacing in grid placement. So the length of degraded diameter AB depends on the angle $\angle BOB'$. Assuming that B and P are the two border tags near B', A choose B to form the key pair only if $|BB'| \leq |PB'|$. Let the central angle $\angle BOP = \theta$, we have $\angle BOB' \leq \theta/2$. So in the following, we calculate the maximal central angle θ determined by two consecutive border tags before we discuss the length of degraded diameters.

As shown in Fig. 7(a) and 7(b), A and B are the consecutive border tags. O is the location of the reader. The central angle is $\theta = \angle AOB$. The arc represents the border of ideal identification region. There are two cases of θ due to different relations between two consecutive border tags.

1) Case 1: as shown in Fig. 7(a), the consecutive border tags are in the same horizonal or vertical line, then $|AB| = d$

$$\begin{aligned} \theta &= \arctan(|AB|/|AO|) \\ &< \arctan(d/(r-d)) \end{aligned} \tag{3}$$

2) Case 2: as shown in Fig. 7(b), the consecutive border tags are in the diagonal line, then $|AB| = \sqrt{2}d$. With law of cosines, we have

$$\begin{aligned} \cos\theta &= \frac{|OA|^2 + |OB|^2 - |AB|^2}{2|OA||OB|} \\ &= \frac{|OA|^2 + |OB|^2 - 2d^2}{2|OA||OB|} \\ (r - d < |OA| \leq r, r - d < |OB| \leq r) \end{aligned} \tag{4}$$

Due to the symmetry structure of this equation, the minimal value of $\cos\theta$ is got when $|OA| = |OB|$:

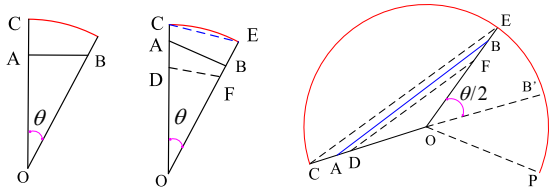

(a) (b) (c)

Fig. 7. Accuracy analysis considering the grid placement.

$$min\cos\theta = \frac{2|OA|^2 - 2d^2}{2|OA||OA|} = 1 - \frac{d^2}{|OA|^2}$$
$$> 1 - \frac{d^2}{(r-d)^2}$$
$$\theta < \arccos(1 - \frac{d^2}{(r-d)^2}) \quad (5)$$

The result in Equation 5 subsumes the one in Equation 3.

As shown in Fig. 7(c), the locations of A and B are bounded by $|CD| = d$ and $|EF| = d$ respectively, $CE//DF$, the length of degraded diameter $|AB|$ can be calculated as follows:

$$|AB| \geq |DF| = \frac{r-d}{r}|CE|$$
$$= 2(r-d)\cos(\frac{\theta}{4})(\theta < \arccos(1 - \frac{d^2}{(r-d)^2})) \quad (6)$$

Then we have the following theorem.

Theorem 5: The length of a degraded diameter is at least $minDD = 2(r-d)\cos(\frac{\theta}{4})(\theta < \arccos(1 - \frac{d^2}{(r-d)^2}))$.

Theorem 5 gives the lower bound of a degraded diameter's length. Based on it, we modify Algorithm 1 to calculate quality index. We relax the condition that two activated tags form a key pair only if the distance between them is greater than $2r$. The threshold $2r$ is changed to $minDD$. However, this relaxation makes the computation of quality index not polynomial solvable. The following is an equivalent formulation and with the complexity of NP-hard. x_{ij} denotes whether tag i and tag j form a key pair ($x_{ij} = 1$) or not ($x_{ij} = 0$). N is the set of border tags. The objective is to find the maximal number of key pairs subject to that each tag can participate in at most one key pair.

$$max \sum_{(i,j)\in N} x_{ij}$$
$$st. \sum_{(i,j)\in N} x_{ij} + \sum_{(j,i)\in N} x_{ij} \leq 1 \quad (7)$$
$$x_{ij} \in \{0,1\}$$

Since the possible length of a degraded diameter is between $2r$ and $minDD$, we propose an iterative heuristic algorithm to compute quality index as in Algorithm 2. We define the threshold of a diameter's length firstly as $2r$ (line 3) and run Algorithm 1 using this threshold (line 5). After that, the threshold is changed to the maximal distance between any two tags in N (line 6). The process repeats until the threshold is less than $minDD$ or all tags are considered (line 4). In the simulation section, we will see that the performance of this algorithm is quite desirable. The worst time complexity of this algorithm is $O(n^3)$.

E. Extension for Pure Radius Loss and Mixed Loss

In this sub-section, we extend the ATI method to pure radius loss and mixed loss.

In pure radius loss, if a key pair still exists in the activated region, ATI can find the exact location of the reader. The difference between it and pure angle loss is that the activated region of the former is larger than the latter. The previous defined quality index is still reasonable since the quality index in this situation is larger than that in corresponding pure angle loss. If a key pair cannot be found in the activated region, the situation is quite complex. However, one special case is easy to solve: the radius loss in all angles is a constant say a. ATI again can find the exact location of the reader. The quality index needs to be revised since if a is large enough no key pair can be found according to Definition 5. We revise the threshold of a diameter's length from $2r$ to $2(r-a)$. This revision ensures that the quality index of a large activated region greater than that of a small activated region, which matches the ground truth. The revision of threshold in Algorithm 2 can also be similarly made here to consider the grid placement.

Algorithm 2: Revised Quality Index Algorithm

```
1 qualityIndex = 0
2 put all border tags in N
3 threshold = 2r
4 while N ≠ ∅ && threshold > minDD do
5 |   run Algorithm 1 line 3-9 replacing 2r in line 5 with
  |   threshold, record all calculated distance |AB| in S
6 |   threshold = max S
7 end
8 return qualityIndex
```

Inspired by the two situations discussed above, we propose a method to address the general case of pure radius loss. The same ATI is used to obtain the localization result. The quality index is defined as the following.

$$a\frac{max\phi'(\theta)}{r}^2 + b\frac{1}{std(\phi'(\theta))} + c * count(max\phi'(\theta)) \quad (8)$$

The quality index depends on three parts. The first part describes the maximum radius loss in all angles. The second part considers the distribution of radius loss. The third part is complementary to the second part and highlights the number of diameters with the length of $max(\phi'(\theta))$ which is the most cogent argument in quality index. a, b, c are system parameters used to adjust the weights of these three parts and their values are learned through experiments.

Mixed loss is a combination of pure angle loss and pure radius loss. The quality index defined in Equation 8 is compatible. Due to limited space, we omit the detailed analysis.

F. Analysis on Real Identification Region

We consider the identification region of real RFID readers, which may not be a perfect circle due to different signal propagation attenuation amounts and different antenna gains in different directions. Our analysis is based on [4]. That work defines an upper bound (R_u) and a lower bound (R_l) of the readers signal transmission range, and a Degree of Irregularity (DOI) denoting maximum variation of the reader's transmission range per unit degree, as shown in Fig. 8.

We have two methods to make our solution applicable to a real identification region. The first method is proposed in [4], to use a low-cost antenna array with multiple radiation elements in

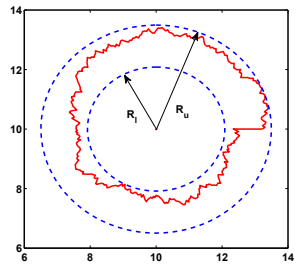

Fig. 8. An example of real identification region ($R_l = 2, R_u = 3.5, DOI = 0.1$)

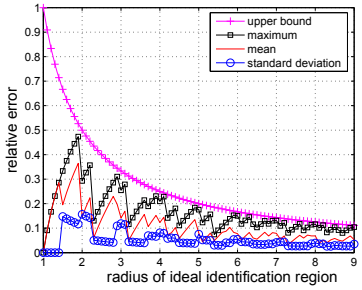

Fig. 9. Localization relative error caused by grid placement (the reader is at grid intersections)

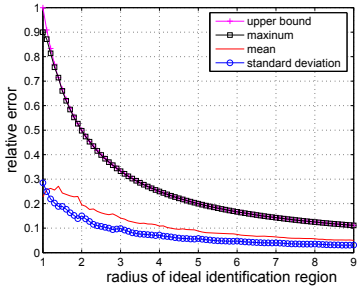

Fig. 10. Localization relative error caused by grid placement (the reader is in a grid cell)

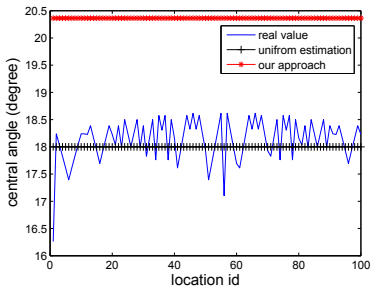

Fig. 11. The maximal central angle determined by two consecutive border tags (radius=5)

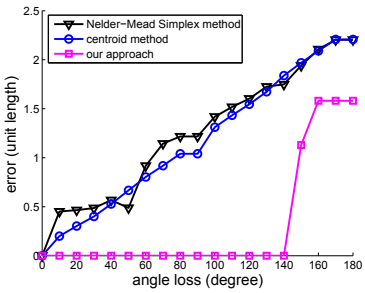

Fig. 12. Localization result in pure angle loss (radius=5, the reader is at grid intersections)

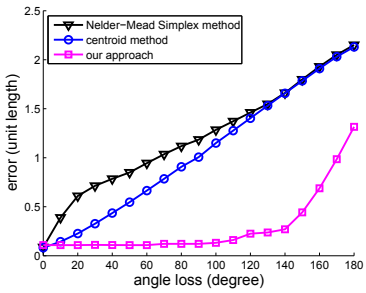

Fig. 13. Localization result in pure angle loss (radius=5, the reader is in a grid cell)

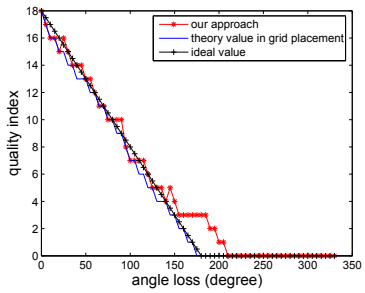

Fig. 14. Quality index in pure angle loss calculated by Algorithm 2 (radius=7)

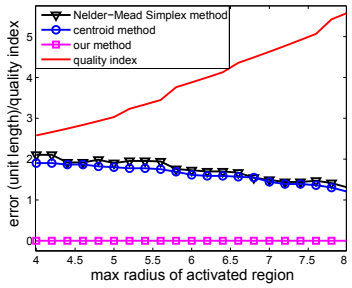

Fig. 15. Localization result and quality index in pure radius loss (radius=10)

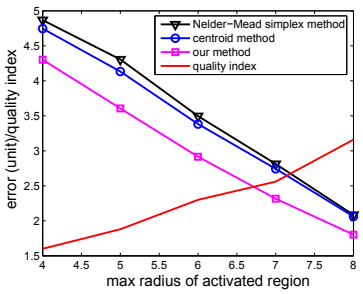

Fig. 16. Localization result and quality index in mixed loss (angle loss=270 degrees, radius=10)

different directions to minimize DOI. If only common antenna at hand, the authors suggest to rotate the antenna to achieve similar effect of the antenna array. During this design, the identification region is quite approximate to a circle. The other method is to compare the ideal identification region with the circle determined by R_u. The process is like our analysis in the regional fault. If the difference is not so significant (e.g. angle loss $< \pi$), we just use this circle to perform localization. Otherwise, we conservatively base on the circle determined by R_l to perform localization.

V. Simulation Results

This section presents our simulation results. The purpose of the simulation has two parts. The first one is to validate the theorems mentioned in previous sections. The second one is to compare our approach with existing approaches in different situations. We choose Nelder-Mead Simplex method [4] and centroid method [9] for comparison. Here we consider missing reading, so the weighted centroid methods which deals with unintended reading is not included. In the accuracy analysis, we also compare our approach with the uniform estimation used in [4].

Without loss of generality, we place the tags in a grid with the spacing of 1 unit length and change the radius of the ideal identification region. The simulation is performed under both the cases that 1) the reader is at grid intersections and 2) the reader is in a grid cell. For the latter, we enumerate all the points using horizontal and vertical step of 0.1 unit length and number these points from 1 to 100.

A. Errors Caused by Grid Placement

We firstly check the errors caused by grid placement. The results are to validate Theorem 4 and Theorem 5.

The relative error of the reader's location caused by grid placement is shown in Fig. 9 and 10. In the former figure the reader is placed at the grid intersection $(0, 0)$ and in the latter figure the reader's location is evenly distributed in the grid cell encompassed by $(0, 0)$,$(0, 1)$, $(1, 0)$ and $(1, 1)$. Due to the symmetry structure of grid, other locations share the same results. In both cases, we enumerate all the border tags to check the error caused by grid placement. We show the maximum, mean and standard deviation of relative error in the figures. We can see that the upper bound of the relative error stated in Theorem 4 (d/r) is strictly obeyed especially when

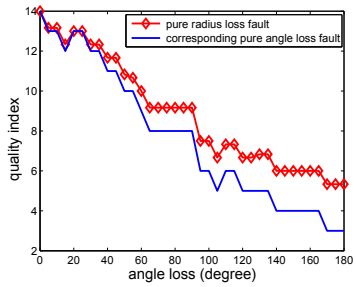

Fig. 17. The comparison of quality index in pure radius loss and corresponding pure angle loss

Fig. 18. Experiment configuration of RFID reader localization in an office

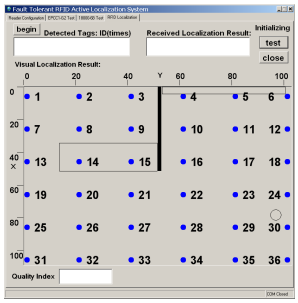

Fig. 19. RFID tag deployment shown in the software GUI

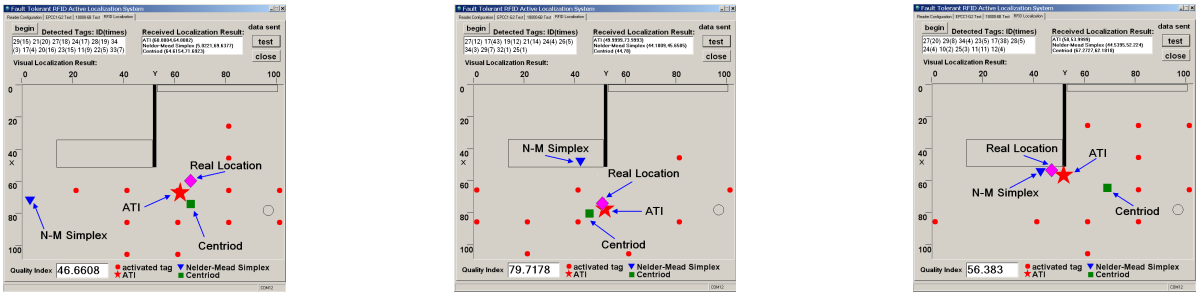

(a) (b) (c)

Fig. 20. Some experiment results of different approaches. The real location of the reader is a)(60,65) b)(50,75) c)(45,55)

the reader is in a grid cell (Fig. 10). When the reader locates at grid intersections, the curve is a zigzag and some kind of periodic (not in strict sense) (Fig. 9). This can be explained by examining the error computation. Since the tags are restricted to grid intersections, the error equation has a floor function in it. When expanding the floor function with Fourier series, there will be a sine function so the result is some kind of periodic.

For the maximal central angle determined by two consecutive border tags, we compare our approach with uniform estimation used in [4] which considers all border tags uniformly distributed in the circle border. We compare them in different radius of ideal identification region, denoted as r. When $r \leq 6$, our result serves as the upper bound for all locations while the uniform estimation cannot (the case $r = 5$ is shown in Fig. 11). When $6 < r \leq 10$ (figure omitted), uniform estimation also can serve as the upper bound and is stricter than our result. However, the result reverses when $r > 10$ (figure omitted). As a general estimation of maximal central angle in different cases, we can safely say that the result of our method is more accurate than that of the uniform estimation method.

B. Performance in Pure Angle Loss

We compare the localization accuracy of our approach, Nelder-Mead Simplex method and centroid method in pure angle loss. According to the results shown in Fig. 12 and 13, our approach is more accurate than the two existing approaches.

When the reader locates at grid intersections, our approach can find the exact location of the reader if the angle loss is less than 135 degrees when radius=5 (Fig. 12) and about 90 degrees when radius=7 (figure omitted). The result is less than 180 degrees proved by Theorem 3, due to the error caused by grid placement. When the reader is distributed in a grid cell, the result is shown in Fig. 13. At the first stage, the result is quite accurate (error<0.1 unit length), and when the angle loss is above a threshold, the error is sharply increased. However, even in the worst case, our approach still has a better result. For a common case of 90 degrees angle loss, the error of ATI is only 10.3% of the Nelder-Mead Simplex method and 12.1% of the centroid method.

Fig. 14 shows the effectiveness of quality index computed by Algorithm 2. The ideal value denotes the quality index in the situation that all border tags evenly locate at the border of ideal identification region. We also show the theory value of quality index in the grid placement. It is computed when the location of the reader is already known. This value is always smaller than the ideal value due to the error caused by grid placement. From the figure, we can see that our approach is quite close to the ideal value in most of cases. Slight deviation occurs near the 180 degrees but is still acceptable.

C. Performance in Pure Radius Loss and Mixed Loss

We check the performance of different methods in pure radius loss and mixed loss. In pure radius loss, if a key pair still exists, the result is similar to the one in pure angle loss. We take extensive simulations to validate this. One case is shown in Fig. 15. When the key pair does not exist, we show a result of mixed loss in Fig. 16, with an angle loss of 270 degrees. In these two cases, we fix $std(\phi'(\theta))$ and change $max(\phi'(\theta))$ (see Equation 8). We also repeat the simulation by fixing $max(\phi'(\theta))$ and changing $std(\phi'(\theta))$, and get similar results. As a result, our approach outperforms the existing two methods. However, we can see that the difference between our approach and the existing ones is not so significant when the angle loss is quite large. Considering moderate faults in practical situations, our approach can get a desirable performance.

We have proposed Equation 8 to compute the quality index in pure radius loss and mixed loss. Here we check whether the computed quality index matches the ground truth. As shown in Fig. 17, we compare the quality index in pure radius loss with the one in corresponding pure angle loss when the angle loss varies from 0 to 180 degrees. The former is always higher than the latter. This fairly matches the ground truth that the activated region in pure radius loss is larger than the one in corresponding pure angle loss. We also check the pure radius loss with constant radius loss in all directions, the result shows that the quality index in a large activated region is higher than the one in a small activated region (figure omitted). In the general case of pure radius loss, we also obtain the results which match the ground truth, as shown in Fig. 15 and 16. All these results show that our definition of quality index is consistent and distinguishes different situations quite well.

VI. Experiments

We developed an RFID reader localization system called RFID-RLS using C# language and preformed experiments in our office, which can be extended to other environments such as the warehouse. Although the experiment itself is simple, we find useful information from it and validate our approach.

The devices include 915 MHz UHF RFID readers and EPC Class 1 Generation 2 UHF RFID tags. The reader has an isotropic antenna. The power of the reader is set to 18 dBm which means a 2.5m reading range in the floor in our experiment. The on-site configuration of the system is shown in Fig. 18. The tags are put into a grid with the spacing of 40cm. Detailed tag placement can be seen in a software GUI (Fig. 19) where walls and desks in the office are also shown as the background. Quality index is shown in the lowest textbox. For ease of comparison, we show the localization results of ATI, Nelder-Mead Simplex method and centroid method together.

We set a time duration of 6 seconds in each localization process for obtaining more reliable raw data. Then the data are fed into the localization component to calculate the result. We observed that the detected tags varied from time to time even the reader was static. This may be caused by environment interference and human activities in the office. The walls and desks also make localization difficult because they can block the paths of radio propagation and cause multipath propagation. For example, the upper-left nine tags (tag 1-3, 7-9 and 13-15 in Fig. 19) failed to be detected during the whole experiment process due to blocking of the wall.

We move the reader around to check the localization results. Some results are shown in Fig. 20(a) to 20(c). In Nelder-Mead Simplex method, we need to rough estimate the object's position before starting the optimization process, which is not easy in practice. Here we use the result of centroid method as the initial position. We find the Nelder-Mead Simplex method is quite unstable. As shown in Fig. 20(a) and 20(b), the result is far from the real location. Especially in Fig. 20(b), the result is under the desk, which may make the user quite confused. The centroid method is relatively stable in the experiments. However, the result of it sometimes is not very accurate. As shown in Fig. 20(c), the localization result of centroid method deviates from the real location. On the contrary, the result of ATI is quite stable and accurate during all the experiments.

The quality index works well in the experiments. When the detected tags scatter more evenly in all directions, the quality index is higher (Fig. 20(b)). When there are more angle loss or radius loss in the activated region, the quality index is lower (Fig. 20(a) and 20(c)).

VII. Conclusion

In this paper, we investigated the RFID reader localization based on passive tags when RFID faults frequently happen. Among all the faults, long-lasting regional fault is the most difficult one to be dealt with. We proposed a method named ATI which can tolerate long-lasting regional fault, and defined quality index to measure localization results. Simulation and experiment results show that our approach outperforms existing approaches in terms of localization accuracy. Moreover, quality index matches the ground truth quite well.

Acknowledgment

This research is partially supported by the Hong Kong RGC (GRF grant PolyU5106/10E and F-HK25/10T), and the China National 973 Project (2009CB320702).

References

[1] S. S. Saad and Z. S. Nakad, "A standalone RFID indoor positioning system using passive tags," *IEEE Tran. Industrial Electronics*, vol. 58, no. 5, pp. 1961–1970, 2011.

[2] H. J. Lee and M. C. Lee, "Localization of mobile robot based on radio frequency identification devices," in *Proc. SICE-ICASE*, 2006, pp. 5934–5939.

[3] M. Bouet and G. Pujolle, "L-VIRT: Range-free 3-D localization of RFID tags based on topological constraints," *Computer Communications*, vol. 32, no. 13-14, pp. 1485–1494, 2009.

[4] C. Wang, H. Wu, and N.-F. Tzeng, "RFID-based 3-D positioning schemes," in *Proc. INFOCOM*, 2007, pp. 1235–1243.

[5] D. Hähnel, W. Burgard, D. Fox, K. Fishkin, and M. Philipose, "Mapping and localization with RFID technology," in *Proc. IEEE International Conference on Robotics and Automation*, 2004, pp. 1015–1020.

[6] T. Sanpechuda and L. Kovavisaruch, "A review of RFID localization: applications and techniques," in *Proc. ECTI-CON*, 2008, pp. 769–772.

[7] L. M. Ni, Y. Liu, Y. C. Lau, and A. P. Patil, "LANDMARC: Indoor location sensing using active RFID," in *Proc. PerCom*, 2003, pp. 407–415.

[8] X. Shen, Z. Wang, P. Jiang, R. Lin, and Y. Sun, "Connectivity and RSSI based localization scheme for wireless sensor networks," in *Proc. ICIC*, 2005, pp. 578–587.

[9] N. Bulusu, J. Heidemann, and D. Estrin, "Gps-less low-cost outdoor localization for very small devices," *Personal Communications*, vol. 7, no. 5, pp. 28–34, 2000.

[10] T. He, C. Huang, B. M. Blum, J. A. Stankovic, and T. Abdelzaher, "Range-free localization schemes for large scale sensor networks," in *Proc. MobiCom*, 2003, pp. 81–95.

[11] Y. Park, J. W. Lee, D. Kim, J. J. Jeong,and S. Kim, "Mathematical formulation of RFID tag floor based localization and performance analysis for tag placement," in *Proc. ICARCV*, 2010, pp. 1–5.

[12] K. Kaemarungsi and P. Krishnamurthy, "Modeling of indoor positioning systems based on location fingerprinting," in *Proc. INFOCOM*, 2004, pp. 1012–1022.

[13] K. Yamano, K. Tanaka, M. Hirayama, E. Kondo, Y. Kimuro, and M. Matsumoto, "Self-localization of mobile robots with RFID system by using support vector machine," in *Proc. IROS*, 2004, pp. 3756–3761.

[14] R.H.Tütüncü, K.C.Toh, and M.J.Todd, (2001, Aug.), "SDPT3 - a Matlab software package for semidefinite-quadratic-linear programming, version 3.0." [Online]. Available: http://www.math.nus.edu.sg/∼mattohkc/